



Thermal accommodation in nanoporous silica for vacuum insulation panels

S. Sonnick^{a,b,*}, M. Meier^b, G. Ünsal-Peter^a, L. Erlbeck^a, H. Nirschl^b, M. Rädle^a

^a CeMOS – Center for Mass Spectrometry and Optical Spectroscopy, Mannheim University of Applied Sciences, Paul-Wittsack-Straße 10, 68163 Mannheim, Germany

^b Institute for Mechanical Process Engineering and Mechanics, Karlsruhe Institute of Technology, Straße am Forum 8, 76131 Karlsruhe, Germany

ARTICLE INFO

Article History:

Received 13 November 2019

Revised 10 December 2019

Accepted 27 December 2019

Available online 10 January 2020

Keywords:

Accommodation coefficient

Thermal conductivity

Coupling effect

Vacuum insulation

Mercury intrusion porosimetry

Gas influence

Pressure influence

ABSTRACT

The thermal accommodation coefficient is a measure for the quality of thermal energy exchange between gas molecules and a solid surface. It is an important parameter to describe heat flow in rarefied gases, for example, in aerospace or vacuum technology. As special application, it plays a decisive role for the thermal transport theory in silica filled vacuum insulation panels. So far, no values have been available for the material pairings of silica and various gases. For that reason, this paper presents thermal conductivity measurements under different gas-pressure conditions for precipitated and fumed silica in combination with the following gases: helium, air, argon, carbon dioxide (CO₂), sulfur dioxide (SO₂), krypton, and sulfur hexafluoride (SF₆). Additionally, a calculation method for determining thermal accommodation coefficients from the thermal conductivity curves in combination with the pore size distribution of silica determined by mercury intrusion porosimetry is introduced. The results are compared with existing models.

© 2020 The Author(s). Published by Elsevier Ltd. This is an open access article under the CC BY-NC-ND license. (<http://creativecommons.org/licenses/by-nc-nd/4.0/>)

1. Introduction

Vacuum insulation panels are high-performance thermal insulations, which offer an extremely high thermal resistance with a very small space requirement. Their function is based on the so-called Knudsen effect, which presupposes that the mean free path length of the gas molecules is in the same order of magnitude as the pore size of the solid structure. By using nanoporous materials such as silica and/or applying a vacuum this can be achieved. In this way it is possible to reduce the amount of heat transferred through the gas phase to a negligible amount. It is well known that the Knudsen model [1] can be used when the gas thermal conductivity in evacuated porous materials is considered [2–4]. This is important when the gas flow is in the transition region, where the pore size x is in the same order of magnitude as the mean free path of the molecules L . There are, however, two difficulties with the calculation of gas thermal conductivity in vacuum insulation panels. The first one is that especially for silica-based materials with spherical particles a strong coupling between the solid and the gaseous thermal conductivity needs to be taken into account. This coupling differs significantly for different silica

materials but can be estimated as a function of the porosity, at least for precipitated silica. That was shown in the previously published paper [5]. The second problem, which is examined in more detail in the present publication is, that the Knudsen model requires the thermal accommodation coefficient (TAC) α . The TAC is a measure for the quality of energy exchange between the gas molecules and the solid surface. In a manner of speaking, it describes the boundary condition for the flow of gas molecules in the slip and transition flow regimes [6]. It was Maxwell [7] who first introduced the idea that a fraction α of gas molecules is remaining in thermal equilibrium with the surface while the remaining part $\alpha - 1$ is scattered. Later, Smoluchowski [8] verified the suggestion experimentally when he found a temperature jump at the solid-gas interface. The term “thermal accommodation coefficient”, however, was first used by Knudsen [1]. He defined it as the relationship between two temperature differences

$$\alpha = \frac{T_1 - T_2}{T_1 - T_2'} \quad (1)$$

where T_1 is the mean temperature of the molecules before colliding with the solid surface and T_2 and T_2' are the temperatures of the molecules scattered and fully accommodated to the surface respectively. Especially for rarefied gases where individual collisions of single gas molecules with the surface are more important than at continuum conditions, the AC is not negligible [9]. Due to the fact that α is a function of many parameters, like the kind of gas, the

* Corresponding author at: CeMOS – Center for Mass Spectrometry and Optical Spectroscopy, Mannheim University of Applied Sciences, Paul-Wittsack-Straße 10, 68163 Mannheim, Germany.

E-mail address: s.sonnick@hs-mannheim.de (S. Sonnick).

Nomenclature

Symbols

d_{kin}	kinetic diameter of molecules, m
f	coupling effect factor, -
k_B	Boltzmann constant, J/K
Kn	Dimensionless Knudsen number, -
L	mean free path of molecules, m
M	molar mass, g/mol
p	pressure, mbar
R	gas constant, J/Kmol
T	temperature, K
V	volume, m ³
x	pore size, m
α	accommodation coefficient, -
β	dimensionless coefficient for gaseous conductivity calculation, -
κ	adiabatic coefficient, -
λ	thermal conductivity, W/mK
λ'	thermal conductivity of a single pore, W/mK
λ_0	free gas thermal conductivity, W/mK
ϕ	porosity, -

Subscripts and abbreviations

c	coupling
g	gaseous
max	maximum / end of intrusion
r	radiative
s	solid
sr	solid and radiative

surface materials, temperature, adsorption effects and surface roughness, it is nearly impossible to find data for every occurring problem. It is well known that thermal accommodation increases with increasing surface roughness, because gas molecules do more than one collision, on the average, before leaving the surface [10]. In addition, an increasing molar mass of the gas molecules leads to an increasing α , because of the lower velocity and therefore longer residence time of the molecules at the surface [11], but the accommodation coefficient is generally independent of the gas pressure [12]. Thus, TACs are reasonably constant for a given gas and surface combination [13]. Some models exist to describe the TAC based on classical mechanics [14–16] or quantum mechanics [17–19], but they either require very detailed information about the solid surface condition [20], which is difficult to access in nanoporous materials, or are only valid for extreme clean surfaces which do not occur in practice. For that reason many authors assume $\alpha = 1$ when calculating gas thermal conductivity in porous silica materials which are filled

with air or rarefied air, for example in vacuum insulation panels [21–23]. The resulting error is not to be neglected. It was shown that in the transition region in particular the gas thermal conductivity increases by approximately 70% if a value of 0.8 instead of 0.1 is used for α [24]. Thus, the goal of this work is to analytically determine TACs especially for different silica materials in combination with different gases like helium, air, argon, carbon dioxide (CO₂), sulfur dioxide (SO₂), krypton, and sulfur hexafluoride (SF₆).

One can find values for individual material pairings in the literature. Some of them are listed in Table 1. Furthermore, Saxena and Joshi [25] collected an extensive compilation of measured TAC values for different material pairings by different authors. The fluctuation of the available values can be due to the different measuring methods but also to minimal differences in the surface quality of the materials or of contaminations on the surfaces. Unfortunately, it is almost impossible to obtain values for different silica materials and especially their inner pore surfaces as they can be found in vacuum insulation panels (VIPs).

2. Thermal transport theory in porous media

Thermal transport in porous media is composed of three main mechanisms: thermal conductivity over the solid backbone of the material λ_s , radiation λ_r and gaseous thermal conductivity λ_g . In a macroscopic surrounding λ_g is almost independent from the gas pressure p because of two mutually cancelling effects. As the pressure decreases, the number of gas molecules involved in heat transfer decreases as well, which would normally reduce thermal conductivity. The second effect is, that at the same time the mean free path increases, causing the individual distances at which the gas particles transport the energy to become larger, which in turn would lead to an improvement of the heat transfer [29]. Both effects happen at the same time when changing the gas pressure in a macroscopic surrounding. The situation changes if the mean free path gets in the same order of magnitude as the representative size scale, which bounds the surrounding room. In this case, the distance at which the energy can be transported in one step is not limited by the mean free path but by the size of the surrounding volume, which for porous materials is the pore size. Hence, the thermal conductivity becomes a function of the gas pressure.

A fourth mechanism which basically depends on the microscopic shape of the material and gas pressure is the coupling effect between solid and gaseous thermal conductivity λ_c [30]. This coupling is negligible for most foams [31] but plays a decisive role for silica based core materials.

This becomes clear when looking at Fig. 1 which shows the different heat transfer mechanisms using the example of two touching spherical particles. Consequently, the thermal conductivity of a silica material can be described as a sum of these four mechanisms as

Table 1
Examples of thermal accommodation coefficients for different solid-gas pairings from the literature.

Solid	Gas	Thermal accommodation coefficient	Measuring method	Temperature [K]	Source
Tungsten (extremely clean surface)	Argon	0.2357	thin filament thermal conductivity cell	308.15	[12]
Silica, fumed	CO ₂	0.45	absorption of the radiation of a Q-switched laser	300	[26]
	NO	0.33			
	Helium	0.385			
Nickel	Krypton	0.965	thin filament thermal conductivity cell	298.15	[10]
	Helium	0.368			
Platinum	Krypton	0.959	concentric spherical shells heat flux measurement	314.5	[27]
	Helium	0.28			
304 stainless steel	Argon	0.85	parallel plates temperature drop measurement	308.15	[28]
	Nitrogen	0.8			
	Argon	0.87			
	Helium	0.36 (machine finish), 0.4 (polished finish)			

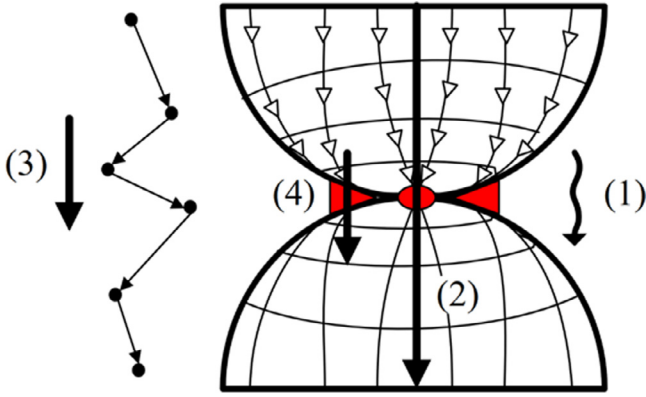


Fig. 1. Heat transfer mechanisms in porous media: radiation λ_r (1), solid thermal conductivity λ_s (2), gas thermal conductivity λ_g (3) and coupling effect λ_c (4), modified from [32].

shown in Eq. (2) [3,31]. All heat transfer mechanisms are temperature dependent, however, in this work constant and steady state temperature is assumed.

$$\lambda(p) = \lambda_s + \lambda_r + \lambda_g(p) + \lambda_c(\lambda_g) \quad (2)$$

In the present case, particular attention must be paid to the gas thermal conductivity, since it is decisive for the determination of the TACs. It can be described with Eq. (7).

$$\lambda_g' = \frac{\lambda_0(T)}{1 + 2 * \beta * Kn} \quad (3)$$

In Eq. (3) [33] λ_0 is the thermal conductivity of the gas at atmospheric pressure and β is a dimensionless coefficient depending on the thermal accommodation coefficient α and the adiabatic coefficient of the gas κ . It can be calculated via Eq. (4) [33]. The adiabatic coefficient is the relationship between specific heat capacity at constant pressure c_p and constant volume c_v .

$$\beta = \frac{5\pi}{32} * \frac{9\kappa - 5}{\kappa + 1} * \frac{2 - \alpha}{\alpha} \quad (4)$$

The dimensionless Knudsen number Kn is the decisive dimensionless parameter for the description of gas thermal conductivities in rarefied gases. It describes the ratio between the mean free path of the gas molecules L and a representative physical length scale. Because the Knudsen model was developed for the case of parallel plates, the physical length scale would be the distance between the plates. In a porous material with almost spherical pores, a correction factor needs to be considered as was mentioned in the previously published paper [5]. The modified equation for the dimensionless Knudsen number is shown in Eq. (5).

$$Kn(p, x) = \frac{6L}{\pi x} \quad (5)$$

Now it is obvious how sensitive the TAC is in terms of gas thermal conductivity. A dependency of gas thermal conductivity plotted over Kn -number on different TACs can be found in [24]. The mean free path L is a function of the gas pressure and the kinetic diameter of the gas molecule. It can be determined according to the kinetic gas theory using Eq. (6)

$$L(p) = \frac{k_B * T}{\sqrt{2} * \pi * d_{kin}^2 * p} \quad (6)$$

with $k_B = 1.38 * 10^{-23} \frac{J}{K}$ as the Boltzmann constant, T as the absolute temperature and d_{kin} as the kinetic diameter of the gas molecules. A molecule can have more than one size characterizing dimension if it is not spherical. The kinetic diameter d_{kin} is the size of the sphere of influence that can lead to a scattering event [34]. It can be calculated

with the kinetic gas theory out of the dynamic viscosity or the thermal conductivity of the gas.

Another model to predict the gas-thermal conductivity, which is considered very similar to the Knudsen model, was proposed by Bourret [35] and is shown in Eq. (7).

$$\lambda_g = \frac{\lambda_g^0}{1 + \frac{\lambda_g^0}{xp} \sqrt{\frac{\pi MI}{2R}}} \quad (7)$$

The decisive difference between this and Knudsen's model is that neither the thermal accommodation coefficient nor the isentropic exponent are taken into account. The type of gas is only considered by the molar mass. It is to be examined whether this is permissible.

Following, if taking into account the pore size distribution of the silica material, which can be measured with mercury intrusion porosimetry, for every pore size x and gas pressure p the dimensionless Knudsen number Kn can be calculated. This results in a matrix of dimensionless Knudsen numbers, which can then be used to determine the gaseous thermal conductivity for every pressure and pore size using Eq. (3).

The overall gaseous thermal conductivity can now be calculated via Eq. (8)

$$\lambda_g(p) = \phi \int \lambda_g' \frac{dV}{V_{max}} dx \quad (8)$$

with dV as the pore volume which refers to the pore size x , V_{max} as the total pore volume of the material and ϕ as the porosity of the silica material.

As previously mentioned, the solid thermal conductivity λ_s and the radiative thermal conductivity λ_r can be assumed to be constant. Thus $\lambda_{sr} = \lambda_s + \lambda_r$ is an offset value, which can be determined by measuring thermal conductivity at a very low pressure level, where λ_g and λ_c are negligible.

The coupling effect was found to be in a linear relationship to the gas thermal conductivity [30,36], so it is possible to introduce a coupling effect factor f , as it is shown in Eq. (9).

$$\lambda_c = \lambda_g * f \quad (9)$$

In order to fit the calculated gas thermal conductivity with the measured ones, e.g. using the least square method, like it was performed in [5], a thermal accommodation coefficient must be assumed. For that reason, the TAC was assumed to have the value "1" for the gas whose molar mass is closest to that of the solid material. Because according to the theory

$$\alpha = \frac{4M_s M_g}{(M_s + M_g)^2} = 1 - \left(\frac{M_s - M_g}{M_s + M_g} \right)^2 \quad (10)$$

the TAC is unity if the molar masses of the colliding gas and solid molecules are equal [33]. In Eq. (10) M_s and M_g are the molar masses of the solid and the gas respectively.

3. Materials and method

For the present investigation, one type of precipitated silica (PS, *co. Grace Germany GmbH*) and one type of fumed silica (FS, *co. Wacker Chemie AG*) are used. Prior to the measurements, the samples have been compressed with 5 bar and dried completely. The samples were heated for about 3 hours at 100°C and an absolute pressure of < 0.1 mbar. They were then stored for longer than 12 h at < 0.1 mbar

For determination of the pore size distribution of the silica materials an "AutoPore III (*co. micromeritics, USA*)" is used.

To measure the thermal conductivity over the gas pressure, a self-constructed guarded hot plate apparatus is used. The sample size is 160 × 160 × ≈ 6 mm. The measurement is conducted with a heating plate temperature of 45°C and a cooling plate temperature of 15°C.

Table 2
Important physical properties of all gases used in the experiments.

Gas name	λ_0 [W/mK] [37]	d_{kin} [nm]	K [-]	M [g/mol]
Helium (He)	0.1536	0.26 [38]	1.67	4.00
Air	0.02625	0.36	1.40	28.96
Argon (Ar)	0.0177	0.34 [39]	1.67	39.95
Carbon dioxide (CO ₂)	0.01705	0.33 [40]	1.29	44.01
Sulfur dioxide (SO ₂)	0.0095	0.36 [39]	1.35	64.06
Krypton (Kr)	0.00949	0.36 [39]	1.67	83.80
Sulfur hexafluoride (SF ₆)	0.0135	0.55 [39]	1.10	146.05

The kinetic diameter of air molecules was calculated as average value from the corresponding individual gases.

Thus, the average temperature is 30°C. More detailed information about the measurement apparatus and the uncertainty analysis for the thermal conductivity measurement as well as a more detailed description of the pore size measurement can be found in [5].

For the measurements under a certain gas atmosphere, first the test bench has to be flooded with the corresponding gas to prevent any influences. Then the vacuum chamber is evacuated in order to record the measuring points from the lowest pressure upwards. The used gases and their physical properties are listed in Table 2.

To determine the coupling effect factor f and the accommodation coefficient α , calculated thermal conductivities need to be fitted to the measurement results with f and α as variables. Because the molar masses of the solid surface SiO₂ and the gas SO₂ are very close to each other, regarding to Eq. (10) it can be assumed that α is maximum for this material pairing. Based on this assumption, alpha was set to unity ($\alpha = 1$) for that special case, knowing that a complete energy transfer is unrealistic. Consequently, the coupling effect factor can be determined by fitting calculated to measured data of SiO₂. The coupling effect is a geometric phenomenon [30] and therefore independent from the kind of gas. Thus, the coupling effect factor determined with SO₂ remains constant for all gases and the TAC can be fitted accordingly. The whole procedure performed to determine the thermal accommodation coefficient of the listed gases and the inner pore walls of silica is presented schematically in Fig. 2.

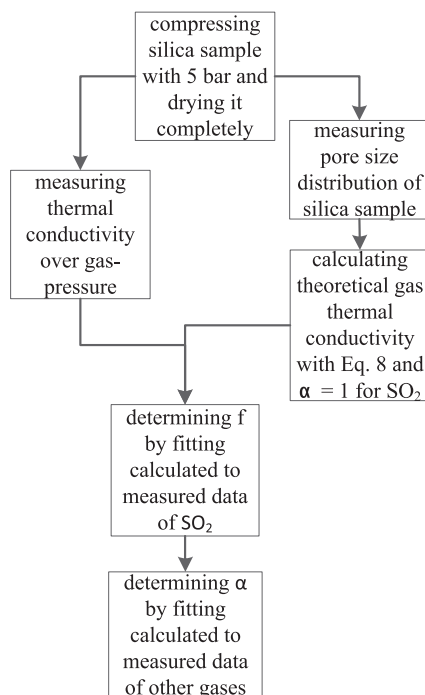


Fig. 2. Flow chart of the performed procedure to determine TACs for different gases.

4. Results and discussion

The porosities ϕ of the silica samples measured with mercury intrusion porosimetry are 0.876 and 0.967 for precipitated and fumed silica respectively. The pore size distributions of both samples are plotted in Fig. 3. As expected, fumed silica shows a higher porosity which is caused by its pearly, open and hierarchic structure compared to precipitated silica which tends to have a bulky and aggregated structure [41]. Their nanopores differ a little. PS and FS show peaks at around 9.4 nm and 12.5 nm respectively.

The sum of the solid thermal conductivity and the radiation λ_{sr} can be measured at very low pressure conditions and has been found to be 0.0051 W/mK for PS and 0.0062 W/mK for FS, both with a standard deviation of 0.0003 W/mK.

Gas thermal conductivity λ_g over gas pressure p curves for all gases are shown in Fig. 4, for PS in the upper graph and FS in the lower graph. In general, it can be stated that gases with a higher thermal conductivity λ_0 show a faster increase in the resulting gas thermal conductivity λ_g with increasing gas pressure and thus normally also higher values at atmospheric pressure. However, it also becomes clear that not only the thermal conductivity but also the molecule diameter and weight play a decisive role. If SF₆ is taken for example, which with 146.05 g/mol is by far the heaviest and with 5.5 Å the largest of all tested gas molecules, it can be seen that the increase is fast in low pressure regions due to the small resulting mean free path of gas molecules. This means that the dimensionless Knudsen number is already very small at relatively low pressures, which leads to the assumption that the gas thermal conductivity is fully developed at lower pressures. Thus, at higher pressure conditions the curve flattens which results in a comparatively low thermal conductivity at atmospheric pressure.

The coupling effect factor f for the tested precipitated and fumed silica material is equal to 3.91 and 0.53 respectively. The resulting thermal accommodation coefficients are listed in Table 3 as well as in Figs. 5 and 1. The factors f and α were determined using the method already described and shown schematically in Fig. 2.

TACs increase with increasing molar mass as long as the gas molecules are of smaller mass than the solid ones and start to decrease again if this point has been exceeded. This totally fits to Kaganer's theory, which is shown in Eq. (10). Because the molar masses of silica (60.08 g/mol) and SO₂ (64.07 g/mol) are very close to each other, this is where the maximum position of the function is located. However, the theory shows higher values than the measurements for all gases. This can have many reasons, but most likely it is because Kaganer's simple formula is more of an estimate since neither a temperature influence nor the surface conditions like roughness or adsorption effects are included. As mentioned, the results are not close to Kaganer's model, but compared to the measurement results listed in Table 1 they seem explainable. If, for example, the result of CO₂ is compared with [26] where the TAC of CO₂ in combination with FS was also measured, the present result (0.48) is fairly close to the literature value (0.45) considering that these are different silica products and measuring methods. It should be noted in the margin that the adsorption of sulfur dioxide on the silica surfaces might cause modifications in the surface behavior. It is well known that surfaces coated with adsorbed gases tend to have higher thermal accommodation coefficients [20,42,43]. Thus, this effect would underline the assumption of a maximum value for the thermal accommodation coefficient of SiO₂ - SO₂. In addition, the measurements for all gases show slightly higher values for precipitated than for fumed silica. This behavior may be related to the hydroxyl groups on the surface of silica particles. Due to their production process in general precipitated silicas have more hydroxyl groups than pyrolytically produced silicas [44]. Surface groups that are not integrated into the amorphous solid structure and are thus more weakly bound tend to increase the accommodation coefficient [45]. This could be the explanation for the

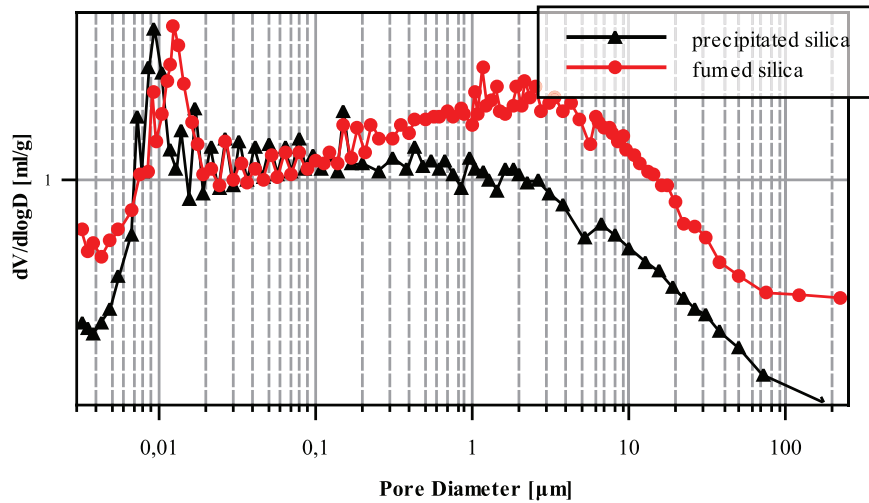


Fig. 3. Pore size distribution of precipitated and fumed silica samples measured with mercury intrusion porosimetry.

higher TACs of precipitated silica. In addition, pyrogenic silica has a higher purity than precipitated silica [46]. Impurities consist mainly of various salts from the wet-chemical precipitation process. If the impurities are regarded as surface contamination, which tends to lead to an increase in the accommodation coefficient [47], this could also be a reason for the higher values.

Another interesting finding from the measurements is the clearly different coupling effect factor f of precipitated and fumed silica. FS has a coupling effect factor of only 0.53 while the PS investigated has a

coupling effect factor of 3.91. That is a result of their different structure in the two to three-digit nanometer range and thus an indication that the coupling effect mainly takes place in this order of magnitude. Both silica types have primary particles around 10 nm. Despite this, as mentioned, their aggregate structure is very different. The two touching spheres pictured in Fig. 1 could be understood to mean that the coupling effect takes place between the primary particles, but this is not correct. The gussets between the primary particles are so small that even at atmospheric pressure there is no gas thermal conductivity and thus no coupling effect between solid and gas thermal conductivity. If one imagines the spherical structure depicted as a spherical aggregate of precipitated silica, however, one understands why the coupling effect factor is greater here than in the case of fumed silica.

Fig. 6 shows a comparison of the present results including thermal accommodation coefficient and coupling effect to the measured data of PS and krypton as an example. Additionally, thermal conductivity calculated with the measured pore size distribution of PS and the model of Bourret [35] are plotted in the graph. One can see that it is not possible to represent the heat transfer in silica samples with this model. It is not expedient to neglect the thermal accommodation coefficient as it depends very much on the substance pairing and does not only correlate with the molar mass of the gas. Supplementing the coupling effect in Bourret's model does not lead to consistent values, although the coupling effect only depends on the geometry of the solid structure. Thus, it should be independent of the type of gas.

Note: Raw data of thermal conductivity measurement as well as pore size distributions are available via "Mendeley Data".

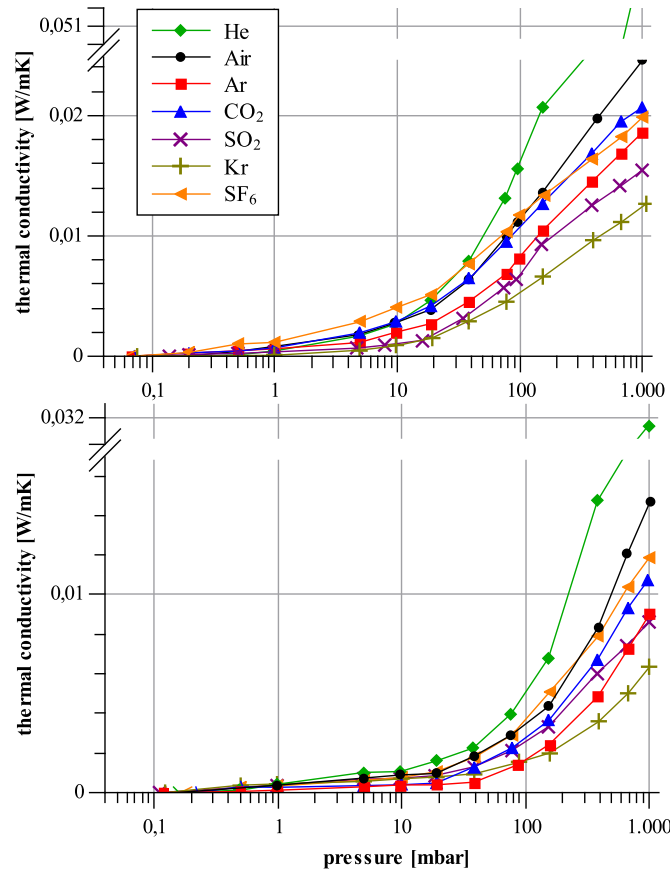


Fig. 4. Gas thermal conductivity of different gases in precipitated silica (upper graph) and fumed silica (lower graph) as a function of the residual gas pressure, y-axis is split between 0.025 and 0.05 W/mK at the upper and between 0.017 and 0.03 W/mK at the lower plot for better legibility.

5. Conclusion

In the presented work thermal conductivity of two silica samples one precipitated and one fumed has been measured under rarefied gas conditions in combination with the gases helium, air, argon, carbon

Table 3
Thermal accommodation coefficients for different silica materials in combination with different gases.

	Precipitated silica	Fumed silica
He	0.12	0.09
Air	0.41	0.33
Ar	0.58	0.32
CO ₂	0.72	0.48
Kr	0.75	0.52
SF ₆	0.43	0.43
SO ₂	1.00	1.00

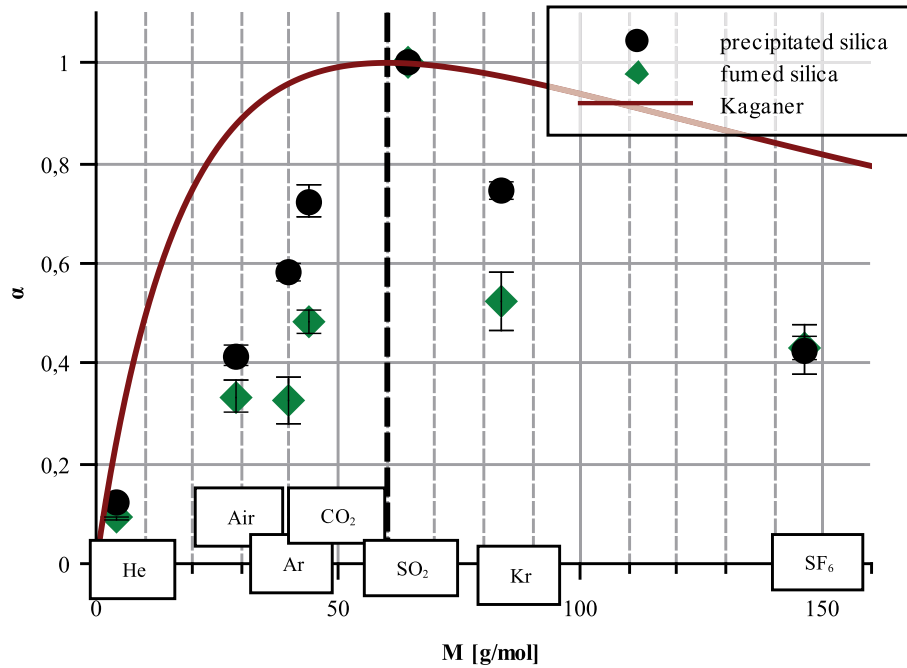


Fig. 5. Thermal accommodation coefficients of different gases with different molar masses compared with the results based on the theory of Kaganer; the dotted vertical line shows the molar mass of the solid material SiO_2 .

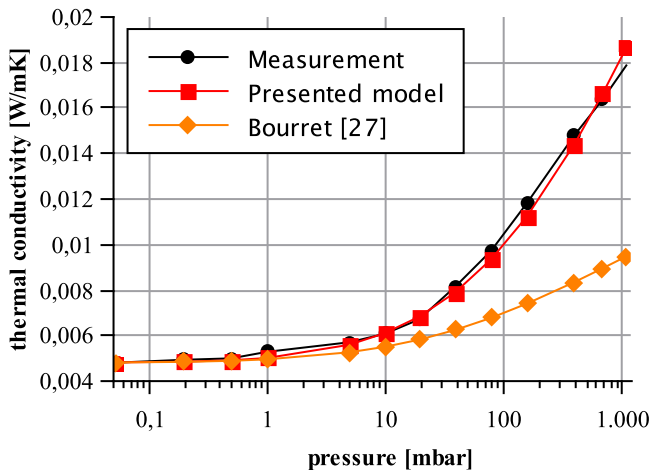


Fig. 6. Comparison of Bourret's [26] model with the presented method of calculation and measured data for precipitated silica and krypton as an example.

dioxide (CO_2), sulfur dioxide (SO_2), krypton, and sulfur hexafluoride (SF_6). The pore size distribution of both samples has been measured with mercury intrusion porosimetry. A calculation procedure is presented to predict gas thermal conductivity as a function of the pore size and gas pressure. In this regard, the coupling between solid and gas thermal conductivity is also taken into account. Furthermore, thermal accommodation coefficients for the inner pore wall-gas boundary layer of silica could be determined experimentally for the first time. The TACs are very important for the complete understanding of the thermal processes in silica materials used for vacuum insulation panels. Until now it was common practice to assume a value of $\alpha = 1$ for air. If one considers the determined result of $\alpha = 0.42$ and $\alpha = 0.32$ for air and precipitated and fumed silica, respectively, it becomes clear that this assumption should be reconsidered. The authors make no claim of total accuracy for the values determined because the values are not measured directly but calculated through measurements of the overall heat flux of the samples. In addition, $\alpha = 1$ was assumed for SO_2 which is certainly not correct in a mathematical sense. On the one hand, the molecular masses of

SO_2 and SiO_2 are not exactly identical and on the other hand, a loss-free energy transfer is rather unlikely even with the same molecular masses of gas and solid surface. Nevertheless, the results have a considerable benefit compared to previous practices in the application of the Knudsen model especially in the field of vacuum insulations. The measurement results for the TACs show an almost linear curve when plotted above the molar mass. They rise with increasing molar mass of the gas up to $M_g = M_s$ and then decrease again linearly with a smaller slope. The basic course is therefore identical to that proposed by Kaganer. In addition, the method presented is compared with a model in which the thermal accommodation coefficient does not occur. It could be shown that the thermal accommodation coefficient cannot be neglected in any case. Furthermore, it was established that the assumption of too high thermal accommodation coefficients leads to an underestimation of the coupling effect. That newly generated findings should be taken into account in future investigations in this field.

Declaration of competing interest

The authors declare that they have no known competing financial interests or personal relationships that could have appeared to influence the work reported in this paper.

Acknowledgments

This work was funded by the Federal Ministry for Economic Affairs and Energy, Germany (AiF Project GmbH) with the grant number 4013931K17 as well as by the Ministry of Science, Research and Arts Baden-Württemberg with the open access publication fund.

References

- [1] M. Knudsen, Die molekulare Wärmeleitung der Gase und der Akkommodationkoeffizient, *Ann. Phys.* 339 (1911) 593–656, doi: [10.1002/andp.19113390402](https://doi.org/10.1002/andp.19113390402).
- [2] M. Bouquerel, T. Duforestel, D. Baillis, G. Rusaouen, Heat transfer modeling in vacuum insulation panels containing nanoporous silicas—a review, *Energy Build.* 54 (2012) 320–336, doi: [10.1016/j.enbuild.2012.07.034](https://doi.org/10.1016/j.enbuild.2012.07.034).
- [3] J. Fricke, U. Heinemann, H.P. Ebert, Vacuum insulation panels—from research to market, *Vacuum* 82 (2008) 680–690, doi: [10.1016/j.vacuum.2007.10.014](https://doi.org/10.1016/j.vacuum.2007.10.014).

- [4] J. Ross-Jones, M. Gaedtke, S. Sonnack, M. Rädle, H. Nirschl, M.J. Krause, Conjugate heat transfer through nano scale porous media to optimize vacuum insulation panels with lattice Boltzmann methods, *Comput. Math. Appl.* (2018), doi: [10.1016/j.camwa.2018.09.023](https://doi.org/10.1016/j.camwa.2018.09.023).
- [5] S. Sonnack, M. Meier, J. Ross-Jones, L. Erlbeck, I. Medina, H. Nirschl, et al., Correlation of pore size distribution with thermal conductivity of precipitated silica and experimental determination of the coupling effect, *Appl. Therm. Eng.* (2019), doi: [10.1016/j.applthermaleng.2019.01.074](https://doi.org/10.1016/j.applthermaleng.2019.01.074).
- [6] A. Agrawal, S.V. Prabhu, Survey on measurement of tangential momentum accommodation coefficient, *J. Vac. Sci. Technol. A* 26 (2008) 634–645, doi: [10.1116/1.2943641](https://doi.org/10.1116/1.2943641).
- [7] J.C. Maxwell, *The Scientific Papers of James Clerk Maxwell*, Dover Publications Inc N. Y., 1890, p. 829.
- [8] M.S. von Smolan, Ueber Wärmeleitung in verdünnten Gasen, *Ann. Phys.* 300 (1898) 101–130, doi: [10.1002/andp.18983000110](https://doi.org/10.1002/andp.18983000110).
- [9] F.O. Goodman, Thermal accommodation, *Prog. Surf. Sci.* 5 (1974) 261–375, doi: [10.1016/0079-6816\(74\)90005-7](https://doi.org/10.1016/0079-6816(74)90005-7).
- [10] I. Amdur, L.A. Guildner, Thermal Accommodation Coefficients on Gas-covered Tungsten, Nickel and Platinum¹, *J. Am. Chem. Soc.* 79 (1957) 311–315, doi: [10.1021/ja01559a018](https://doi.org/10.1021/ja01559a018).
- [11] K.J. Daun, G.J. Smallwood, F. Liu, Investigation of thermal accommodation coefficients in time-resolved laser-induced incandescence, *J. Heat Transf.* (2008) 130, doi: [10.1115/1.2977549](https://doi.org/10.1115/1.2977549).
- [12] L.B. Thomas, C.L. Krueger, S.K. Loyalka, Heat transfer in rarefied gases: critical assessments of thermal conductance and accommodation of argon in the transition regime, *Phys. Fluids* 31 (1988) 2854, doi: [10.1063/1.866994](https://doi.org/10.1063/1.866994).
- [13] S.A. Schaaf, Mechanics of rarefied gases, *Handb. Phys.* 3 (1963) 591–624, doi: [10.1007/978-3-662-10109-4_5](https://doi.org/10.1007/978-3-662-10109-4_5).
- [14] F.O. Goodman, H.Y. Wachman, Formula for thermal accommodation coefficients, *J. Chem. Phys.* 46 (1967) 12.
- [15] R.M. Logan, Calculation of the energy accommodation coefficient using the soft-cube model, *Surf. Sci.* 15 (1969) 387–402, doi: [10.1016/0039-6028\(69\)90131-9](https://doi.org/10.1016/0039-6028(69)90131-9).
- [16] B. Baule, Theoretische Behandlung der Erscheinungen in verdünnten Gasen, *Ann. Phys.* 349 (1914) 145–176, doi: [10.1002/andp.19143490908](https://doi.org/10.1002/andp.19143490908).
- [17] J.M. Jackson, N.F. Mott, R.H. Fowler, Energy exchange between inert gas atoms and a solid surface, *Proc. R. Soc. Lond. Ser. Contain. Pap. Math. Phys. Character* 137 (1932) 703–717, doi: [10.1098/rspa.1932.0166](https://doi.org/10.1098/rspa.1932.0166).
- [18] J.R. Manson, Simple model for the energy accommodation coefficient, *J. Chem. Phys.* 56 (1972) 3451–3455, doi: [10.1063/1.1677719](https://doi.org/10.1063/1.1677719).
- [19] F.O. Goodman, J.D. Gillerlain, Rejection of the devonshire theory of accommodation coefficients in gas–surface interactions (Including a correction for bound state transitions), *J. Chem. Phys.* 57 (1972) 3645–3648, doi: [10.1063/1.1678821](https://doi.org/10.1063/1.1678821).
- [20] S. Song, M.M. Yovanovich, Correlation of thermal accommodation coefficient for “engineering” surfaces, *ASME HTD* 69 (1987) 107–116.
- [21] J. Fricke, H. Schwab, U. Heinemann, Vacuum insulation panels – exciting thermal properties and most challenging applications, *Int. J. Thermophys.* 27 (2006) 1123–1139, doi: [10.1007/s10765-006-0106-6](https://doi.org/10.1007/s10765-006-0106-6).
- [22] U. Heinemann, Influence of water on the total heat transfer in ‘evacuated’ insulations, *Int. J. Thermophys.* 29 (2008) 735–749, doi: [10.1007/s10765-007-0361-1](https://doi.org/10.1007/s10765-007-0361-1).
- [23] R. Coquard, D. Quenard, Modeling of heat transfer in nanoporous silica – influence of moisture, in: 8th Int. Vac. Insul. Symp., Würzburg, Germany, 2007, p. 13.
- [24] D. Bayer, A new facility for the experimental investigation on nano heat transfer between gas molecules and ceramic surfaces, in: 32nd Int. Therm. Conduct. Conf., Indiana USA, 2014, p. 8.
- [25] S.C. Saxena, R.K. Joshi, *Thermal Accommodation and Adsorption Coefficients of Gases*, Hemisphere Pub. Corp., New York, 1989.
- [26] L. Doyennette, M. Margottin–Maclou, H. Gueguen, A. Carion, L. Henry, Temperature dependence of the diffusion and accommodation coefficients in nitrous oxide and carbon dioxide excited into the (00¹) vibrational level, *J. Chem. Phys.* 60 (1974) 697–702, doi: [10.1063/1.1681095](https://doi.org/10.1063/1.1681095).
- [27] H. Yamaguchi, M.T. Ho, Y. Matsuda, T. Niimi, I. Graur, Conductive heat transfer in a gas confined between two concentric spheres: From free-molecular to continuum flow regime, *Int. J. Heat Mass Transf.* 108 (2017) 1527–1534, doi: [10.1016/j.ijheatmasstransfer.2016.12.100](https://doi.org/10.1016/j.ijheatmasstransfer.2016.12.100).
- [28] D.J. Rader, J.N. Castañeda, J.R. Torczynski, T.W. Grasser, W.M. Trott, Measurements of Thermal Accommodation Coefficients, Sandia National Laboratories, 2005, doi: [10.2172/876357](https://doi.org/10.2172/876357).
- [29] P.W. Atkins, J. de Paula, *Wärmeleitung*, Phys. Chem., John Wiley & Sons, 2006, pp. 672–673.
- [30] K. Swimm, S. Vidi, G. Reichenauer, H.-P. Ebert, Coupling of gaseous and solid thermal conduction in porous solids, *J. Non-Cryst. Solids* 456 (2017) 114–124, doi: [10.1016/j.jnoncrysol.2016.11.012](https://doi.org/10.1016/j.jnoncrysol.2016.11.012).
- [31] G. Reichenauer, U. Heinemann, H.-P. Ebert, Relationship between pore size and the gas pressure dependence of the gaseous thermal conductivity, *Colloids Surf. Physicochem. Eng. Asp* 300 (2007) 204–210, doi: [10.1016/j.colsurfa.2007.01.020](https://doi.org/10.1016/j.colsurfa.2007.01.020).
- [32] S. Parzinger, Analytische Modellierung der temperatur- und gasdruckabhängigen effektiven Wärmeleitfähigkeit von Pulvern, Technische Universität München, 2014.
- [33] M.G. Kaganer, Thermal insulation in cryogenic engineering, Israel Program for Scientific Translations (1969).
- [34] G. Joos, I.M. Freeman, *Theoretical Physics*, Courier Corporation, 1986.
- [35] F. Bourret, Mesure de la diffusivité thermique de mousses de carbone par la méthode flash et modélisation de la conductivité thermique radiative, Université de Dijon (1995).
- [36] K. Swimm, G. Reichenauer, S. Vidi, H.-P. Ebert, Impact of thermal coupling effects on the effective thermal conductivity of aerogels, *J. Sol Gel Sci. Technol.* 84 (2017) 466–474, doi: [10.1007/s10971-017-4437-5](https://doi.org/10.1007/s10971-017-4437-5).
- [37] D2 Stoffwerte von bedeutenden reinen Fluiden, in: V. e V (Ed.), VDI-Wärmeatlas, Springer, Berlin Heidelberg, 2013, pp. 175–356. http://link.springer.com/referenceworkentry/10.1007/978-3-642-19981-3_12. (accessed March 20, 2017).
- [38] S. Matteucci, Y. Yampolskii, B.D. Freeman, I. Pinnau, Transport of gases and vapors in glassy and rubbery polymers, *Mater. Sci. Membr. Gas Vap. Sep.*, John Wiley & Sons, Ltd, 2006, pp. 1–47, doi: [10.1002/047002903X.ch1](https://doi.org/10.1002/047002903X.ch1).
- [39] D.W. Breck, Zeolite Molecular Sieves: Structure, Chemistry and Use, John Wiley & Sons Inc, 1974 <https://www.abebooks.de/9780471099857/Zelolite-Molecular-Sieves-Structure-Chemistry-0471099856/plp>. (accessed September 10, 2019).
- [40] A.F. Ismail, K. Khulbe, T. Matsuura, Gas Separation Membranes: Polymeric and Inorganic, Springer International Publishing, 2015, <https://www.springer.com/book/9783319010946>. (accessed September 10, 2019).
- [41] M. Meier, S. Sonnack, E. Asylbekov, M. Rädle, H. Nirschl, Multi-scale characterization of precipitated silica, *Powder Technol.* 354 (2019) 45–51, doi: [10.1016/j.powtec.2019.05.072](https://doi.org/10.1016/j.powtec.2019.05.072).
- [42] J.K. Roberts, The adsorption of hydrogen on tungsten, *Math. Proc. Camb. Philos. Soc.* 30 (1934) 74–79, doi: [10.1017/S030500410001241X](https://doi.org/10.1017/S030500410001241X).
- [43] Isao Yasumoto, Accommodation coefficients of helium, neon, argon, hydrogen, and deuterium on graphitized carbon, *J. Phys. Chem.* 91 (1987) 4298–4301, doi: [10.1021/j100300a019](https://doi.org/10.1021/j100300a019).
- [44] E. Guesnet, B. Bénane, D. Jauffrès, C.L. Martin, G.P. Baeza, G. Foray, et al., Why fumed and precipitated silica have different mechanical behavior: contribution of discrete element simulations, *J. Non-Cryst. Solids* 524 (2019) 119646, doi: [10.1016/j.jnoncrysol.2019.119646](https://doi.org/10.1016/j.jnoncrysol.2019.119646).
- [45] J.W. Lu, W.A. Alexander, J.R. Morris, Gas–surface energy exchange and thermal accommodation of CO₂ and Ar in collisions with methyl, hydroxyl, and perfluorinated self-assembled monolayers, *Phys. Chem. Chem. Phys.* 12 (2010) 12533–12543, doi: [10.1039/B921893A](https://doi.org/10.1039/B921893A).
- [46] Fumed silica and Precipitated silica-Anten Chemical Co., Ltd., (n.d.). <http://www.antenchem.com/en/News/Silicas-Technology/FumedSilicaandPrecipitatedSilica.html>. (accessed December 10, 2019).
- [47] W.M. Trott, D.J. Rader, J.N. Castañeda, J.R. Torczynski, M.A. Gallis, L.A. Gochberg, Experimental determination of thermal accommodation coefficients for microscale gas-phase heat transfer, in: Am. Vac. Soc. 54th Int. Symp., Seattle, WA, 2007.